PHILOSOPHICAL TRANSACTIONS OF THE ROYAL SOCIETY A MATHEMATICAL, PHYSICAL & ENGINEERING SCIENCES

Experiments of the Richtmyer–Meshkov instability

Katherine Prestridge, Gregory Orlicz, Sridhar Balasubramanian and B. J. Balakumar

Phil. Trans. R. Soc. A 2013 **371**, 20120165, published 21 October 2013

PHILOSOPHICAL TRANSACTIONS OF THE ROYAL SOCIETY A

rsta.royalsocietypublishing.org

Review

Cite this article: Prestridge K, Orlicz G, Balasubramanian S, Balakumar BJ. 2013 Experiments of the Richtmyer–Meshkov instability. Phil Trans R Soc A 371: 20120165. http://dx.doi.org/10.1098/rsta.2012.0165

One contribution of 13 to a Theme Issue 'Turbulent mixing and beyond: non-equilibrium processes from atomistic to astrophysical scales II'.

Subject Areas:
mechanical engineering

Keywords:
shock-induced turbulence, mixing, instability, experiments

Author for correspondence:
Katherine Prestridge
e-mail: kpp@lanl.gov

Royal Society Publishing
Informing the science of the future

Experiments of the Richtmyer–Meshkov instability

Katherine Prestridge, Gregory Orlicz, Sridhar Balasubramanian and B. J. Balakumar

Physics Division, Los Alamos National Laboratory, Los Alamos, NM 87545, USA

The Richtmyer–Meshkov instability is caused by a shock interacting with a density-stratified interface. The mixing of the fluids is driven by vorticity created by the interaction of the density and pressure gradients. Because the flow is shock driven, the ensuing mixing occurs rapidly, making experimental measurements difficult. Over the past 10 years, there have been significant improvements in the experimental techniques used in shock-driven mixing flows. Many of these improvements have been driven by modelling and simulation efforts, and others have been driven by technology. High-resolution measurements of turbulence quantities are needed to advance our understanding of shock-driven flows, and this paper reviews the current state of experimental diagnostics, as well as paths forward in studying shock-driven mixing and turbulence.

1. Background

Significant new measurements of mixing in Richtmyer–Meshkov (RM) flows have been made since the review of the instability theory, computations and experiments in 2002 [1]. Shock-driven instabilities and mixing have been studied in many different experimental configurations, ranging from the weak shock regime to highly compressible, turbulent regimes. Generally, as the driver Mach number, *Ma*, and overall speed of the flow increase, it becomes more difficult to measure important flow parameters, such as the density distribution and the mean and fluctuating velocities. Over the past decade, the RM instability has been studied in shock tubes [2], drop tanks [3], laser-driven capsules [4] and explosively driven systems [5]. These experiments illustrate the breadth of scales and Mach

numbers that are experimentally accessible as well as the limitations of the experimental diagnostics as the driver Mach numbers are increased.

Limitations in diagnostics, along with the need to understand some fundamental behaviours about RM instability flows, caused experimentalists to focus for many decades on making integral measurements of the largest scales of mixing. This gave scientists the ability to make generalizations about the growth rate of the mixing region over time. As our ability to simulate these complex, shock-driven flows improves [6,7], experimental measurements that enable us to validate simulations and inform us about the finer scales of mixing in the flow are required.

The initial driver for mixing in RM unstable flows is the baroclinic deposition of vorticity at the interface between the two fluids. In examining the vorticity equation (equation (1.1)), it is clear that the early-time evolution of the flow will be dominated by the baroclinic term (last term in equation (1.1)).

$$\frac{\partial \boldsymbol{\omega}}{\partial t} = -\boldsymbol{u} \cdot \nabla \boldsymbol{\omega} + \boldsymbol{\omega} \cdot \nabla \boldsymbol{u} - \boldsymbol{\omega}(\nabla \cdot \boldsymbol{u}) + \frac{1}{\rho^2} \nabla \rho \times \nabla p. \tag{1.1}$$

If we examine the other terms in equation (1.1), the advection term is relatively small for these flows, but the stretching term increases over time as more three-dimensional mixing effects come into play. If compressibility effects are low, then the dilatation term will be small, but it is still unclear when these effects will become important. The first velocity field measurements and first large-scale vorticity measurements were made about a decade ago in RM flows using particle image velocimetry (PIV) [8], with more vorticity measurements since then [9]. Since that time, the spatial resolution has increased for both velocity measurements using PIV [10] and density measurements using planar laser induced fluorescence (PLIF) [11].

Although great improvements have been made in experimental diagnostics, we are at the nascent stages of application of these methods to a variety of RM flows to understand mixing down to the smallest scales. The effects of variation of Mach number, perturbations in the initial conditions, changing the relative densities of the two gases (Atwood number, $A = (\rho_2 - \rho_1)/(\rho_2 + \rho_1)$), and three-dimensional effects have yet to be discerned. This paper describes our current level of understanding of the impact of these parameters on mixing in RM flows based upon experimental measurements. The focus will be on shock tube and related laboratory-scale experiments, because these have produced the highest resolution measurements of mixing thus far.

2. Mach number effects

Several experiments have been performed to examine the effect of increasing Mach number on RM mixing. While these experiments are an obvious first step, they are not a simple one. In a shock tube, as you increase the driver pressure, the resultant shock speed will increase. In ideal conditions, a pressure ratio of 1.5 is needed to create a Mach 1.2 shock. Owing to losses, usually this ratio is higher. For example, in the shock tube at Los Alamos, the ratio is about two. For a Mach 5 shock in air, the ideal pressure ratio is 29. Very high pressures and shock speeds have the potential to damage weaker portions of the shock tube, for example, the glass windows. Some advantage can be gained by changing the driver gas but it remains difficult to go to very high shock speeds and still capture the time evolution of the flow, so most shock tube experiments are performed with $Ma \leq 3$ for the driver shock.

Many measurements of the mixing width of RM interfaces over various Mach number ranges have been made using schlieren imaging, PLIF, and other light sheet diagnostics. The mixing width is the largest scale of mixing in the flow, and it is dominated by the vorticity deposited at the initial interface [12–15]. Mixing zone width measurements for $Ma \leq 2$ show that growth rates are independent of shock and reshock strength when the widths are plotted as a function of distance travelled [16,17]. The University of Wisconsin shock tube group has done an extensive parametric study of Atwood and Mach number effects on membraneless initial conditions for $Ma \leq 3$, confirming that mix widths can be collapsed with downstream distance [15,18].

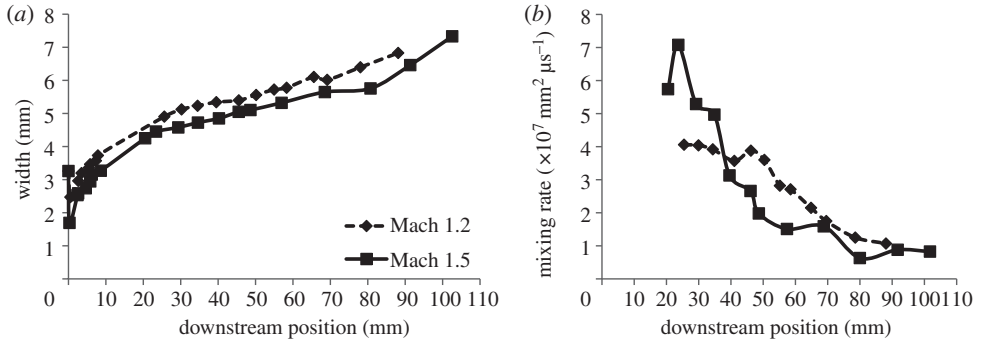

Figure 1. (*a*) Mixing width versus downstream position for Mach 1.2 and 1.5 shock-accelerated heavy gas curtain experiments. Growth rates are the same for each case, with slight offset owing to higher compressions at the higher Mach number. (*b*) Mixing rate versus downstream position for two Mach numbers, showing steeper density gradients at early times for the higher Mach number case.

From the past few decades of experiments, it is clear that mixing width scales with Mach number. One could conclude from this that low Mach number experiments can be performed, and the results can be scaled up to higher Mach configurations. Higher Mach number experiments, such as $Ma > 5$, found in explosively driven flows, inertial confinement fusion capsules and gun-driven experiments, have diagnostic access that is limited to quantities such as mixing widths and possibly mean density in the mixing zone. It is also difficult to make time-resolved measurements under these conditions. As mixing width and mean density are measurements of the largest scales in the flow, it is not possible to determine how mixing and transition scale with Mach number through those measurements alone, and higher resolution mixing measurements are necessary.

A study of Mach effects on small-scale mixing by the Los Alamos shock tube team [17] showed that although growth rates will scale with Mach number, the mixing rate, as measured by the gradients in the density field, is larger at initial higher Mach numbers. Figure 1 shows both the growth rate comparison for two Mach numbers, as well as the mixing rate comparison, where mixing rate is defined as $D(\nabla\rho \cdot \nabla\rho)$, and D is the average diffusivity of the gases [19]. High-resolution density-field images (figure 2) show that while the growth rates of the curtains are similar for two different Mach numbers, the small-scale mixing behaviour is not the same.

Full understanding of the mixing in shock-driven flows is not complete without measurements of the smallest mixing scales. The role of Mach number in introducing compressibility effects the influence the turbulent mixing is unclear. To understand this effect, very high-resolution velocity-field measurements are needed. The requirements for these measurements are discussed in the last section.

3. Initial condition effects

The parametric analysis of Mach number effects cannot be completed unless the initial conditions of the flow are incorporated into the mixing analysis. Recent numerical, theoretical and experimental work has suggested that initial conditions play a more important role in mixing transition than originally thought [20–25] and that even in late times of the mixing evolution, the memory of the initial conditions is not lost [26,27]. Most of the fluid mixing in RM flows occurs owing to the nonlinear growth of the instability; however, this growth is very dependent upon initial conditions that dominate the vorticity deposition and subsequent mixing.

Early shock tube experiments were influenced by initial conditions that used a membrane to separate the gas interface. Recent work has shown disagreement between simulation and experiment when the shock moves from a light gas to a heavy gas, and the gases are separated by a membrane [28]. Techniques that form initial conditions without membranes are a good step towards understanding the impact of initial conditions on late-time mixing structures [13].

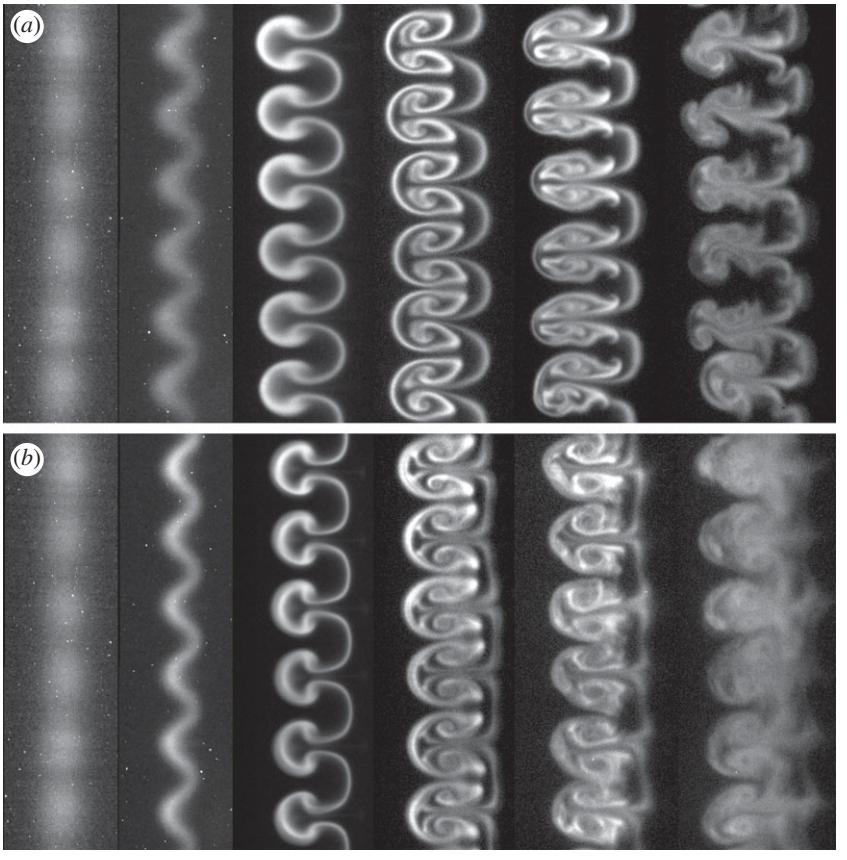

Figure 2. Two time series of PLIF density images of shocked SF_6 gas curtains from the Los Alamos horizontal shock tube. Series (*a*) is Mach 1.2, and from left to right $t = 0, 65, 265, 515, 715, 915$ μs. Series (*b*) is Mach 1.5, $t = 0, 30, 115, 225, 315, 415$ μs. Times for each series have been chosen to match when normalized with advection speed, so downstream positions are $x = 0, 7, 28, 54, 76, 100$ mm for both sequences.

While some experiments have been performed to look at the early-time evolution of RM mixing with different initial interface conditions, at this point in time, we have very little experimental information about smaller scale mixing or about how the modes present in the initial conditions impact either transition or any late-time mixing behaviour. These types of experiments require careful documentation of the initial conditions of each experiment.

Studies of two different wavelength initial conditions were performed at the University of Arizona shock tube laboratory [29] and these studies examined the large-scale mixing of the flow, determining that the mixing widths were able to collapse to a model developed by Sadot [30]. Conversely, studies at the Wisconsin shock tube, under a range of Atwood and Mach numbers, were unable to collapse the mixing width data onto a single curve [31]. This effect was theorized to be the result of changes in the initial conditions, as observed in their earlier work [32]. Experiments at the Ben Gurion University shock tube determined that the amplitude of initial perturbations had some impact on mixing, but that the growth still followed a model based on vorticity deposition at the interface [33].

Measurements that vary reshock timing on the single-mode heavy gas curtain experiments at the Los Alamos shock tube show the impact that the modes in the interface have on the late-time, small-scale mixing [34]. In figure 3, two interfaces with very different modes are shocked, and the late-time density-field images show variation in the mixing behaviours. More detailed analysis of the small-scale mixing is required to understand the nature of the mixing at late times. This will require high spatial resolution velocity- and density-field measurements.

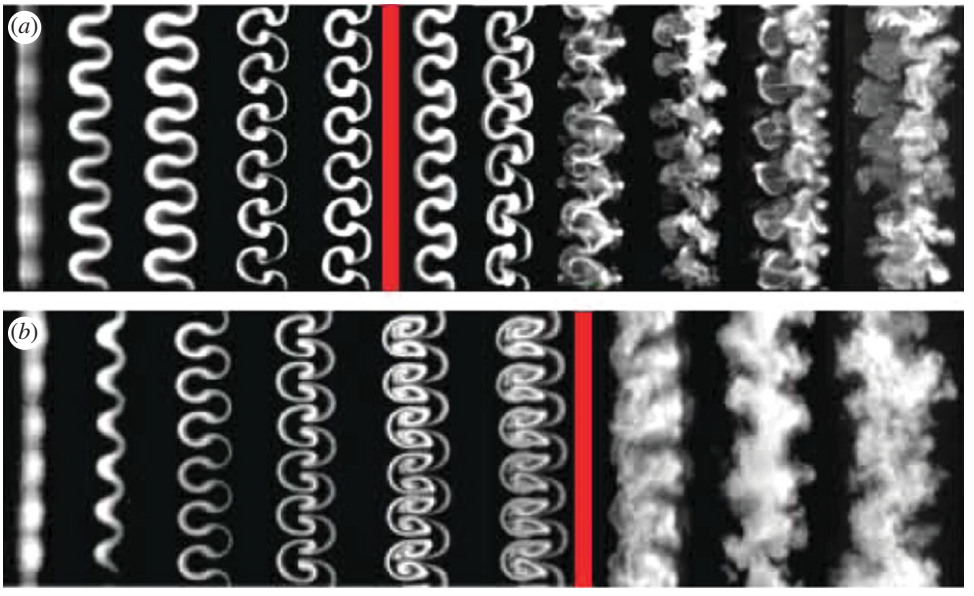

Figure 3. Density-field images of two different gas curtain experiments. Image (*a*) is a time series of 0, 150, 180, 230, 280, reshock just after 280 (vertical bar), 285, 290, 355, 430, 480, 530 μs, times relative to first shock passage through initial conditions. Image (*b*) is a time series of 0, 90, 260, 360, 510, 560, reshock at 600 (vertical bar), 660, 810, 910 μs. (Online version in colour.)

4. Atwood number effects

Another important influence on fluid mixing is the density difference between the two fluids. The most recent studies of Atwood number effects have come from the Wisconsin shock tube [18,31] and the Polytech Marseille shock tube [35]. In these studies, the gases were changed and the orientation of the interface with respect to the shock was also changed, with positive Atwood number indicating that the shock moves from light to heavy gas and negative indicating heavy to light. In both cases, the mixing widths and growth rates are compared to growth rate models [36,37] and good agreement is found. No comprehensive study of the effects of Atwood number on small-scale mixing has been made.

5. Three-dimensional effects

Some experiments have been designed with three-dimensional perturbations on the initial interface, for the purpose of understanding how three-dimensional effects impact the growth rates and how fully three-dimensional flows can be modelled [38,39]. Work at the Ben Gurion shock tube visualized mixing widths for two- and three-dimensional initial conditions, with single- and multi-mode perturbations, for two different Atwood numbers. They found different growth rates for each mode of a multi-mode initial condition when compared with the single-mode initial conditions [40]. These results are substantiated with work by Chapman & Jacobs [41] using a drop tower and three-dimensional 'egg crate' perturbations on the initial interface. Mixing widths are determined using a three-dimensional vortex deposition model, but more nonlinear growth is seen in the three-dimensional case when compared with the two-dimensional case [41]. Higher spatial resolution density-field information, including measurements at later times, would assist in determining how best to model multi-mode growth of three-dimensional flows.

Convergent shock tubes [42], annular shock tubes [43] and shocked gas bubbles [44,45] have shown some trends in overall mixing width development, including possible suppression of the growth of shocked gas bubbles owing to the outer soap film containment [46]. Increased growth

of the mixing zone was found in the convergent tube studies. In these cases, the membranes separating the gases caused so much light scattering that they blocked the signal of the tracer particles [47]. Experiments in more complex flow geometries appear to be plagued by diagnostic difficulties and the challenges in setting up the non-planar drivers make this class of experiments very difficult.

6. Future directions

There is currently no comprehensive understanding of the nature of shock-driven mixing from the initial deposition of baroclinic vorticity at the density interface, to the smallest mixing scales of the flow. In non-equilibrium flows such as this, there is a strong reliance upon experimental data to inform the modelling and simulation efforts. As modelling and simulations demand more information about vorticity, enstrophy, mixing fractions and turbulence quantities, such as Reynolds stress terms and velocity–density cross-correlations, it becomes more critical that measurements of mean and fluctuating density and velocity fields be made [48]. Density–velocity correlations and Reynolds stress terms have been measured only using simultaneous PIV–PLIF at the Los Alamos shock tube [10], and more measurements of turbulence quantities have recently been made [49]. Many more turbulence measurements are needed for the many different flow configurations described above. The impact of initial conditions, three-dimensional effects, driver-shock Mach number and Atwood number can be determined only using measurements that are sensitive enough to reflect the mixing at the smallest scales. And there are presently no effective temperature or pressure field diagnostics that can be implemented in these high-speed flows.

Some of today's diagnostics can be reasonably extended up to Mach 5 regimes, but the time- and length-scale measurement requirements pose challenges. For example, shock of $Ma = 5$ has a velocity behind it of about $1400\,\mathrm{m\,s^{-1}}$. Expected velocity fluctuations in the accelerated flow are about 20% of this velocity, or $u_\eta = 280\,\mathrm{m\,s^{-1}}$. If one assumes a reasonable length scale of eddies in the flow of about $\eta = 0.01\,\mathrm{m}$, then $Re_\eta = 900\,000$ in air. Estimates of the Taylor scale are $\lambda = 2\eta\sqrt{Re_\eta} = 0.7\,\mathrm{mm}$, and the Kolmogorov length scale of $L_\mathrm{K} = \eta/Re_\eta^{3/4} = 0.3\,\mu\mathrm{m}$. Approximate eddy turnover times for this flow would be $\tau_\eta = L_\mathrm{K}^2/\nu = 38\,\mathrm{ns}$.

These flow parameter estimates put several constraints upon diagnostics. Holographic techniques have the spatial resolution to measure the Taylor microscale, with current technologies possibly having resolutions of $10\,\mu\mathrm{m}$ [50]. Hotwires are unreliable for estimating velocity or density in even low Mach number flows [51]. Laser Doppler velocimetry (LDV), with a finite measurement volume, allows resolution of the Taylor microscale, so it is useful for a quick understanding of the nature of the mean and fluctuating velocities at a point in the flow. However, LDV is a point-measurement system that does not allow a comprehensive understanding of non-equilibrium mixing. The current best spatial resolutions in PLIF are about $50\,\mu\mathrm{m}$; however, there are some concerns about the application of acetone PLIF to higher Mach number flows, where the fluorescent response of the acetone is no longer linear, and dissociation of the acetone will occur [52]. For the higher Mach number cases, a different density-field diagnostic will have to be used.

In planar PIV, the basic technology used currently is a doubled Nd:YAG laser with two power supplies, so that the 10 ns light pulses can be controlled independently in time. For a Mach 1.2 shock wave, a typical pulse separation is $2\,\mu\mathrm{s}$, and with 2 megapixel charge-coupled device cameras, this results in a resolution of approximately $150\,\mu\mathrm{m}$ per velocity vector. For our Mach 5 example case, with velocities behind the shock that are 10 times that of the Mach 1.2 case, our time between pulses would have to be approximately 200 ns. The actual pulse width of the laser would create approximately 1 pixel of motion blur, adding to the PIV error, and cameras with an interframe time of 200 ns are needed. This configuration is a definite possibility given existing technologies but it is stretching the capability. A large advantage of PIV is that the image processing is not computationally intensive.

If research in the RM community can continue to make progress in both spatial and temporal resolution of measurements, we may be able to understand enough of the physics of these unsteady flows to extrapolate to higher Mach numbers. This will require that close collaborations among experimentalists, theoreticians and numerical physicists continue.

Funding statement. This work was supported by the Department of Energy under contract no. DE-AC52-06NA25396.

References

1. Brouillette M. 2002 The Richtmyer–Meshkov instability. *Annu. Rev. Fluid Mech.* **364**, 445–468. (doi:10.1146/annurev.fluid.34.090101.162238)
2. Collins B, Jacobs, J. 2002 PLIF flow visualization and measurements of the Richtmyer–Meshkov instability of an air/SF6 interface. *J. Fluid Mech.* **464**, 113–136. (doi:10.1017/S0022112002008844)
3. Niederhaus CE, Jacobs JW. 2003 Experimental study of the Richtmyer–Meshkov instability of incompressible fluids. *J. Fluid Mech.* **485**, 243–277. (doi:10.1017/S002211200300452X)
4. Zhou Y *et al*. 2003 Progress in understanding turbulent mixing induced by Rayleigh–Taylor and Richtmyer–Meshkov instabilities. *Phys. Plasmas* **10**, 1883–1896. (doi:10.1063/1.1560923)
5. Zellner MB, Buttler WT. 2008 Exploring Richtmyer–Meshkov instability phenomena and ejecta cloud physics. *Appl. Phys. Lett.* **93**, 114102. (doi:10.1063/1.2982421)
6. Grinstein F. 2009 On integrating large eddy simulation and laboratory turbulent flow experiments. *Phil. Trans. R. Soc. A* **367**, 2931–2945. (doi:10.1098/rsta.2009.0059)
7. Kawai S, Shankar S, Lele S. 2010 Assessment of localized artificial diffusivity scheme for large-eddy simulation of compressible turbulent flows. *J. Comput. Phys.* **229**, 1739–1762. (doi:10.1016/j.jcp.2009.11.005)
8. Prestridge K, Vorobieff P, Rightley P, Benjamin R. 2000 Validation of an instability growth model using particle image velocimetry measurements. *Phys. Rev. Lett.* **84**, 4353–4356. (doi:10.1103/PhysRevLett.84.4353)
9. Aure R, Jacobs JW. 2008 Particle image velocimetry study of the shock-induced single mode Richtmyer–Meshkov instability. *Shock Waves* **18**, 161–167. (doi:10.1007/s00193-008-0154-x)
10. Balasubramanian S, Orlicz GC, Prestridge KP. 2013 Experimental study of initial condition dependence on turbulent mixing in shock-accelerated Richtmyer–Meshkov fluid layers. *J. Turbul.* **14**, 170–196. (doi:10.1080/14685248.2013.792932)
11. Tomkins C, Kumar S, Orlicz G, Prestridge K. 2008 An experimental investigation of mixing mechanisms in shock-accelerated flow. *J. Fluid Mech.* **611**, 131–150. (doi:10.1017/S0022112008002723)
12. Hecht J, Alon U, Shvarts D. 1994 Potential flow models of Rayleigh–Taylor and Richtmyer–Meshkov bubble fronts. *Phys. Fluids* **6**, 4019–4030. (doi:10.1063/1.868391)
13. Jacobs JW, Jenkins DG, Klein DL, Benjamin RF. 1995 Nonlinear growth of the shock-accelerated instability of a thin fluid layer. *J. Fluid Mech.* **295**, 23–42. (doi:10.1017/S00221209500187X)
14. Zhang Q, Sohn S. 1997 An analytical nonlinear theory of Richtmyer–Meshkov instability. *Phys. Fluids* **9**, 1106–1124. (doi:10.1063/1.869202)
15. Motl B, Oakley J, Ranjan D, Weber C, Anderson M, Bonazza R. 2009 Experimental validation of a Richtmyer–Meshkov scaling law over large density ratio and shock strength ranges. *Phys. Fluids* **21**, 126102. (doi:10.1063/1.3280364)
16. Leinov E, Malamud G, Elbaz Y, Levin LA, Ben-Dor G, Shvarts D, Sadot O. 2009 Experimental and numerical investigation of the Richtmyer–Meshkov instability under re-shock conditions. *J. Fluid Mech.* **626**, 449–475. (doi:10.1017/S0022112009005904)
17. Orlicz GC, Balakumar BJ, Tomkins CD, Prestridge KP. 2009 A Mach number study of the Richtmyer–Meshkov instability in a varicose, heavy-gas curtain. *Phys. Fluids* **21**, 064102. (doi:10.1063/1.3147929)
18. Motl BJ, Niederhaus JHJ, Ranjan D, Oakley JG, Anderson MH, Bonazza R. 2007 Experimental study for ICF-related Richtmyer–Meshkov instabilities. *Fusion Sci. Technol.* **52**, 1079–1083.
19. Buch KA, Dahm WJA. 1998 Experimental study of the fine-scale structure of conserved scalar mixing in turbulent shear flows. Part 2. *J. Fluid Mech.* **364**, 1–29. (doi:10.1017/S0022112098008726)

20. Dimonte G. 2004 Dependence of turbulent Rayleigh–Taylor instability on initial perturbations. *Phys. Rev. E* **69**, 056305. (doi:10.1103/PhysRevE.69.056305)
21. Miles AR, Edwards MJ, Greenough JA. 2005 Effects of initial conditions on compressible mixing in supernova-relevant laboratory experiments. *Astrophys. Space Sci.* **298**, 17–24. (doi:10.1007/s10509-005-3907-3)
22. Goncharov VN, Gotchev OV, McCrory RL, McKenty PW, Meyerhofer DD, Sangster TC, Skupsky S, Cherfils-Clerouin C. 2006 Ablative Richtmyer–Meshkov instability: theory and experimental results. *J. Phys. IV* **133**, 123–127. (doi:10.1051/jp4:2006133024)
23. Balakumar BJ, Orlicz GC, Tomkins CD, Prestridge KP. 2008 Dependence of growth patterns and mixing width on initial conditions in Richtmyer–Meshkov unstable fluid layers. *Phys. Scripta* **T132**, 014013. (doi:10.1088/0031-8949/2008/T132/014013)
24. Miles AR. 2009 The blast-wave-driven instability as a vehicle for understanding supernova explosion structure. *Astrophys. J.* **696**, 498–514. (doi:10.1088/0004-637X/696/1/498)
25. Thornber B, Drikakis D, Youngs DL, Williams RJR. 2010 The influence of initial conditions on turbulent mixing due to Richtmyer–Meshkov instability. *J. Fluid Mech.* **654**, 99–139. (doi:10.1017/S0022112010000492)
26. George W. 2006 Recent advancements towards the understanding of turbulent boundary layers. *AIAA J.* **44**, 2435–2449. (doi:10.2514/1.19951)
27. Banerjee A, Andrews M. 2009 3D simulations to investigate initial condition effects on the growth of Rayleigh–Taylor mixing. *Int. J. Heat Mass Transf.* **52**, 3906–3917. (doi:10.1016/j.ijheatmasstransfer.2009.03.032)
28. Mariani C, Vandenboomgaerde M, Jourdan G, Souffland D, Houas L. 2008 Investigation of the Richtmyer–Meshkov instability with stereolithographed interfaces. *Phys. Rev. Lett.* **100**, 254503. (doi:10.1103/PhysRevLett.100.254503)
29. Jacobs JW, Krivets VV. 2005 Experiments on the late-time development of single-mode Richtmyer–Meshkov instability. *Phys. Fluids* **17**, 034105. (doi:10.1063/1.1852574)
30. Sadot O, Erez L, Alon U, Oron D, Levin L, Erez G, Ben-Dor G, Shvarts D. 1998 Study of nonlinear evolution of single-mode and two-bubble interaction under Richtmyer–Meshkov instability. *Phys. Fluids Lett.* **80**, 1654–1657. (doi:10.1103/PhysRevLett.80.1654)
31. Weber C, Motl B, Oakley J, Anderson M, Bonazza R. 2009 Richtmyer–Meshkov parameter study. *Fusion Sci. Technol.* **56**, 460–464.
32. Puranik PB, Oakley JG, Anderson MH, Bonazza R. 2004 Experimental study of the Richtmyer–Meshkov instability induced by a Mach 3 shock wave. *Shock Waves* **13**, 413–429. (doi:10.1007/s00193-004-0231-8)
33. Sadot O, Rikanati A, Oron D, Ben-Dor G, Shvarts D. 2003 An experimental study of the high Mach number and high initial-amplitude effects on the evolution of the single-mode Richtmyer–Meshkov instability. *Laser Part. Beams* **21**, 341–346. (doi:10.1017/S0263034603213082)
34. Balasubramanian S, Orlicz G, Prestridge K, Balakumar B. 2012 Experimental study of initial condition dependence on Richtmyer–Meshkov instability in the presence of reshock. *Phys. Fluids* **24**, 034103. (doi:10.1063/1.3693152)
35. Jourdan G, Houas L. 2005 High-amplitude single-mode perturbation evolution at the Richtmyer–Meshkov instability. *Phys. Rev. Lett.* **95**, 204502. (doi:10.1103/PhysRevLett.95.204502)
36. Sadot O, Erez L, Alon U, Oron D, Levin L, Erez G, Ben-Dor G, Shvarts D. 1998 Study of nonlinear evolution of single-mode and two-bubble interaction under Richtmyer–Meshkov instability. *Phys. Rev. Lett.* **80**, 1654–1657. (doi:10.1103/PhysRevLett.80.1654)
37. Mikaelian KO. 2003 Explicit expressions for the evolution of single-mode Rayleigh–Taylor and Richtmyer–Meshkov instabilities at arbitrary Atwood numbers. *Phys. Rev. E* **67**, 026319. (doi:10.1103/PhysRevE.67.026319)
38. Vetter M, Sturtevant B. 1995 Experiments on the Richtmyer–Meshkov instability of an air/SF_6 interface. *Shock Waves* **4**, 247–252. (doi:10.1007/BF01416035)
39. Gregoire O, Souffland D, Gauthier S. 2005 A second-order turbulence model for gaseous mixtures induced by Richtmyer–Meshkov instability. *J. Turbul.* **6**, 1–20. (doi:10.1080/14685240500307413)
40. Yosef-Hai A, Sadot O, Kartoon D, Oron D, Levin LA, Sarid E, Elbaz Y, Ben-Dor G, Shvarts D. 2003 Late-time growth of the Richtmyer–Meshkov instability for different Atwood numbers and different dimensionalities. *Laser Part. Beams* **21**, 363–368. (doi:10.1017/S0263034603213112)

41. Chapman PR, Jacobs JW. 2006 Experiments on the three-dimensional incompressible Richtmyer–Meshkov instability. *Phys. Fluids* **18**, 074101. (doi:10.1063/1.2214647)
42. Holder DA, Smith AV, Barton CJ, Youngs DL. 2003 Shock-tube experiments on Richtmyer–Meshkov instability growth using an enlarged double-bump perturbation. *Laser Part. Beams* **21**, 411–418. (doi:10.1017/S0263034603213197)
43. Hosseini SHR, Takayama K. 2005 Experimental study of Richtmyer–Meshkov instability introduced by cylindrical shock waves. *Phys. Fluids* **17**, 084101. (doi:10.1063/1.1964916)
44. Ranjan D, Anderson M, Oakley J, Bonazza R. 2005 Experimental investigation of a strongly shocked gas bubble. *Phys. Rev. Lett.* **94**, 184507. (doi:10.1103/PhysRevLett.94.184507)
45. Sadot O, Levy K, Yosef-Hai A, Cartoon D, Elbaz Y, Srebro Y, Ben-Dor G, Shvarts D. 2005 Studying hydrodynamic instability using shock-tube experiments. *Astrophys. Space Sci.* **298**, 305–312. (doi:10.1007/s10509-005-3951-z)
46. Layes G, Jourdan G, Houas L. 2009 Experimental study on a plane shock wave accelerating a gas bubble. *Phys. Fluids* **21**, 074102. (doi:10.1063/1.3176474)
47. Kumar S, Hornung HG, Sturtevant B. 2003 Growth of shocked gaseous interfaces in a conical geometry. *Phys. Fluids* **15**, 3194–3208. (doi:10.1063/1.1608011)
48. Latini M, Schilling O, Don WS. 2007 High-resolution simulations and modeling of reshocked single-mode Richtmyer–Meshkov instability: comparison to experimental data and to amplitude growth model predictions. *Phys. Fluids* **19**, 024104. (doi:10.1063/1.2472508)
49. Balakumar B, Orlicz G, Ristorcelli J, Balasubramanian S, Prestridge K, Tomkins C. 2012 Turbulent mixing in a Richtmyer–Meshkov fluid layer after reshock: velocity and density statistics. *J. Fluid Mech.* **696**, 67–93. (doi:10.1017/jfm2012.8)
50. Orlov SS, Abarzhi SI, Oh SB, Barbastathis G, Sreenivasan KR. 2010 High-performance holographic technologies for fluid-dynamics experiments. *Phil. Trans. R. Soc. A* **368**, 1705–1737. (doi:10.1098/rsta.2009.0285)
51. Schwaederle L, Mariani C, Jourdan G, Houas L, Haas JF. 2007 Shock-induced mixing zone characterization: an attempt by hot-wire diagnostic. *Shock Waves* **17**, 203–207. (doi:10.1007/s00193-007-0105-y)
52. Thurber M, Hanson R. 1999 Pressure and composition dependences of acetone laser-induced fluorescence with excitation at 248, 266, and 308 nm. *Appl. Phys. B* **69**, 229–240. (doi:10.1007/s003400050799)